Calibration of the simulation parameters of jujubes in dwarfing and closer cultivation in Xinjiang during harvest period

Shiqi Yao[1,2], Gaokun Shi[1,2], Baoshuai Wang[1,2], Huijie Peng[1,2], Hewei Meng[1,2], Za Kan[1,2*]

(1. *College of Mechanical Electrical Engineering, Shihezi University, Shihezi 832000, Xinjiang, China*;
2. *Key Laboratory of Northwest Agricultural Equipment, Ministry of Agriculture and Rural Affairs, Shihezi 832000, Xinjiang, China*)

Abstract: In order to obtain accurate contact parameters of jujubes in dwarfing and closer cultivation in Xinjiang during the harvest period, based on the Hertz-Mindlin (no-slip) contact model in EDEM, the contact parameters, including the coefficient of restitution, static friction, and rolling friction, between jujube and machine components have been calibrated through physical and simulation test. The coefficient of restitution, static friction, and rolling friction between the jujubes and steel (jujube-steel) were calculated as 0.33, 0.46, and 0.04, respectively. The coefficient of restitution, static friction, and rolling friction between the jujubes and polyvinyl chloride (PVC) (jujube-PVC) were calculated as 0.39, 0.61, and 0.06, respectively. The optimum contact parameters among jujubes (inter-jujubes) were 0.23, 0.33, and 0.04. The accumulation test was applied for comparing the simulation and testing values of jujube's repose angle. In the results, the relative error was 1.27% which means the discrete element model and the contact parameters of jujube can be used for the discrete element simulation test. In addition, the results can be adequately used to simulate particle scale mechanics (grain commingling, flow/motion, forces, etc.) of jujube in harvest as well as the design and working mechanism study of post-harvest processing machinery and devices.

Keywords: jujube, EDEM, contact parameter, experiment, calibration
DOI: 10.25165/j.ijabe.20221502.6006

Citation: Yao S Q, Shi G K, Wang B S, Peng H J, Meng H W, Kan Z. Calibration of the simulation parameters of jujubes in dwarfing and closer cultivation in Xinjiang during harvest period. Int J Agric & Biol Eng, 2022; 15(2): 256–264.

1 Introduction

Jujube is one of the major cash crops in southern Xinjiang. In 2018, the yield of jujube in southern Xinjiang has reached nearly 50% of the total yield in China[1]. The development of the jujube industry will promote farmers' income and increase the efficiency of agriculture in southern Xinjiang. Jujube harvest is a particularly important process in jujube production, the research on its technique and equipment is still in an exploratory stage in recent years[2-5]. With the development and application of computer technology, effective numerical simulation can break through the limitation of the traditional physical test as well as reduce the trial production time and cost of the test prototype[6-8]. The discrete element method (DEM) is the most attractive numerical simulation and analysis method, used by researchers to successfully design, analyze and optimize systems and equipment for processing granular materials[9-11]. DEM is used in different fields ranging from mining[12,13] to agriculture[14,15] and post-harvest[16,17], soil-tool interaction[18-20] and so on. In the numerical simulation, an accurate set of material input parameter values is necessary needed[21,22]. The accuracy of the model parameters directly affects the reliability of the simulation test results. The model parameters include the intrinsic parameters (Young's modulus, shear modulus, Poisson's coefficient, and particle density), which can be generated directly by reference or experiments. While the contact characteristics parameter (coefficient of restitution and friction coefficient) and the contact model parameter from the selected embedded contact model (Johnson-Kendall-Roberts surface energy, damping coefficient, and rigidity coefficient between particles in Hysteretic Spring Contact Model) are always calibrated by simulation because they are difficult to obtain directly[23-25].

Recently, focusing on agricultural bulk materials with different physical properties and planting conditions, many researchers simulated and calibrated the contact parameter between material and its contact part based on different embedded contact models in EDEM. Ghodki et al.[26] calibrated the contact parameters of DEM between soybean particles as well as between soybean and acrylic through the testing and simulation on the angle of repose; Gonzalez-Montellan et al.[27] tested the contact parameters of DEM between particles as well as between particle and contact materials focusing on maize grains and olives and used standard spherical particles (glass beads) for comparison as well; Ghodki et al.[28] calibrated the contact parameters of black pepper seeds by numerical simulation and experiment. The flow characteristics of black pepper seeds in precooler and grinder by EDEM have been studied as well; Zhang et al.[29] used orthogonal method to calibrate the contact parameters required by discrete element simulation of maize stalk crushing process; Liu et al.[30] used the Hertz-Mindlin contact model to combine staging test and virtual simulation test, the DEM parameters of mini potato were calibrated; Wang et al.[31] invented a method to establish a mathematical regression model by the active search for the target parameters to calibrate the friction

Received date: 2020-07-06 **Accepted date:** 2022-01-24
Biographies: Shiqi Yao, PhD candidate, research interests: modern agricultural equipment. Email: 442489430@qq.com; **Gaokun Shi**, PhD candidate, research interests: modern agricultural equipment. Email: 1014951940@qq.com; **Baoshuai Wang**, PhD candidate, research interests: modern agricultural equipment. Email: 982056776@qq.com; **Huijie Peng**, MS, research interests: Industrial Engineering and Management, Email: 779642214@qq.com. **Hewei Meng**, Professor, PhD supervisor, research interests: research on modern agricultural equipment. Email: mhw_mac@shzu.edu.cn.
***Corresponding author: Za Kan**, Professor, PhD supervisor, research interests: modern agricultural equipment. College of Mechanical Electrical Engineering, Shihezi University, Shihezi 832000, Xinjiang, China. Tel: +86-993-2055009, Email: kz-shz@163.com.

coefficient between maize seeds particles; Yu et al.[32] built a DEM model of *Panax notoginserg* seed based on a bonded particles model, the contact parameters between *Panax notoginserg* seed as well as between pseudo-ginseng and ABS plastics were calibrated respectively; Lu et al.[33] calibrated the simulated contact parameters of rice bud seeds under different moisture contents by using friction angle test, and the verification test of friction angle from different varieties of rice bud seed has been completed as well; Liao et al.[34] used the contact model of Hertz-Mindlin and HertzMindlin with bonding, according to particle accumulation test and bending destruction test, the simulation contact parameters of fodder crop rape stalk, and the main parameters from crushing simulation model were calibrated and verified respectively; Hao et al.[35] established a bimodal distribution model in EDEM in order to illustrate the physical properties of Chinese yam, according to drop and friction angle test, the contact parameters between sandy loam/Chinese yam and sandy soil as well as between Chinese yam and steel plate are calibrated; Han et al.[36] established the DEM model of ellipsoid brown rice particle and calibrated the rolling friction coefficient of inter-particles through the accumulation test; Shi et al.[37] predicted the rolling friction coefficient in the same shape maize model and the mixture of two different shape maize models respectively, according to the physical and simulation test of repose angle.

In a word, in order to obtain accurate contact parameters in EDEM simulation, the researchers combined simulated and physical test by different embedded contact models, the contact parameters of different agricultural bulk materials was calibrated. It will provide valuable information for further research such as applying DEM analysis on interaction mechanisms between agricultural bulk materials as well as agricultural machine components. However, there is limited research on building the DEM model of jujube and calibrating on contact parameters. Therefore, in order to establish the effective numerical simulation for jujube mechanized harvest process, study the interaction mechanism of movement as well as contact mechanical characteristics between jujube and harvest machine components in the further research, and provide the criterion for the development of jujube harvest machine and its equipment, it has to study on building DEM model of jujube and calibrating of DEM contact parameters.

In this study, the jujube during the harvest period has been applied for research. The angle of repose of jujube-jujube and the contact parameters of jujube-material have been measured. Based on Hertz-Mindlin (no-slip) which is the default contact model in EDEM that simulates without considering adhesion, contact parameters have been simulated and corrected according to the experiment. Meanwhile, based on the angle of repose of jujube as the response value, the contact parameters of inter-jujubes have been calibrated. And a second-order response model between the angle of repose and contact parameters was constructed, in order to provide theoretical support on studying the interaction between jujube and machine components by using EDEM in future research, promoting the mechanized harvest process of jujube to some extent.

2 Materials and methods

2.1 Materials

The jujubes in drafting and closer cultivation during the harvest period, in late October 2019, were collected from the standard test garden of Shihezi University in Xinjiang Production & Construction Corp as the test sample. The water content of the jujube samples was 24.06%, measured by Sartorius MA45 moisture meter (mass measurement accuracy 0.001 g, moisture content measurement accuracy 0.01%).

In order to ensure the accuracy of the DEM model, the three-dimensional size (width-*a*, thickness-*b*, length-*c*, as shown in Figure 1) of 500 jujubes was measured by Vernier calipers (precision is 0.02 mm). Due to the morphological characteristics of jujubes being elliptical, the sphericity was applied for classification. The jujube geometry could be divided as spheroid (sphericity>0.85) and ellipsoid (sphericity<0.85). Furthermore, based on the value of length, ellipsoid particles could be separated as large elliptical particles (a>30 mm) and small elliptical particles (a≤30 mm). The proportion of these three types is 10.4%, 35.4%, and 54.2% respectively.

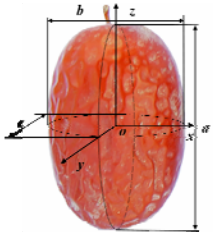

Note: *a* is the width, mm; *b* is the thickness, mm; *c* is the length, mm.

Figure 1 Three-dimensional size schematic diagram of jujube

2.2 Methods

Applying high-speed video and image processing technology, the drop test, sliding/rolling test, and cylinder lifting test were conducted, and the contact parameters (coefficient of restitution, static friction coefficient, rolling friction coefficient) between jujube and contact component (steel, polyvinyl chloride (PVC)) and angle of repose of jujube have been measured respectively. The DEM model of jujube was established according to its shape feature. Based on Hertz-Mindlin (no-slip) contact model in EDEM, combined with the physical test, the simulation and calibration has been completed for the coefficient of restitution and static friction coefficient between jujube and contact component, i.e., the calibrated parameter of jujube-material was defined as the independent variable and the test factor was defined as evaluating indicator. According to obtained evaluation index at different factors in simulation, the curve fitting equation was built up. The result of the test as the target value in the simulation was calculated in the fitting equation to solve the contact parameters, and the simulation was completed for validation. Meanwhile, based on the method of optimization analysis on response surface Box-Behnken, applying angle of repose as response value, the second-order response model between the angle of repose and contact parameters was constructed. In addition, the physical test result was used as a fitting target to obtain the optimal contact parameter combination of inter-jujubes. By comparing and analyzing the relative error between measured results and calibrated simulation results of repose angle, the reliability of the contact parameters of the DEM simulation model was quantitatively evaluated.

3 Physical test

3.1 Jujube-material coefficient of restitution

The coefficient of restitution reflects the degree of conservation of kinetic energy following a collision between particles or between particles and the contact material. The coefficient of restitution is normally defined as the ratio of the post

to the pre-collision normal velocities and the value can be obtained using Equation (1)[38,39].

$$e=\frac{v'}{v} \tag{1}$$

where, e is the coefficient of restitution; v' is the normal relative separation velocity of the contact points of the two objects after the collision, m/s; v is the normal relative proximity velocity of the contact point of the two objects before the collision, m/s.

In this present work, the determination of e was based on drop tests. The test apparatus used allows collisions to be produced between a particle and a soleplate surface. The process was recorded by a high-speed camera (FASTEC-TS4, Fastec Imaging, USA) and the data was processed by ProAnalyst, which is shown in Figure 2. In all assays, two types of material were used as the soleplate surface: steel and PVC. The mass of the jujube is far less than that of the soleplate, the collision will not affect the speed of the soleplate, so the normal velocity component of the panel before and after the collision is 0. It was assumed that energy was conserved before and after impact. The value of e could therefore be expressed as a function of H and h, as shown in Equation (2).

$$e_j=\frac{v_j'}{v_j}=\frac{\sqrt{2gh}}{\sqrt{2gh}}=\frac{\sqrt{h}}{\sqrt{H}} \tag{2}$$

where, e_j is the coefficient of restitution of jujube; v_j' is the normal relative separation velocity of the contact points of the jujube after the collision with the plate, m/s; v_j is the normal relative proximity velocity of the contact point of the jujube before the collision with the plate, m/s. H is the released height, mm; h is the bounced height, mm; g is the gravitational acceleration, g= 9.8 m/s^2.

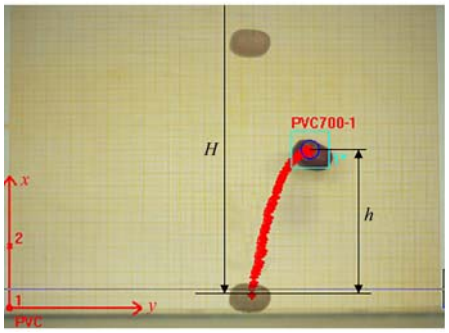

Note: H is the released height, mm; h is the bounced height, mm.

Figure 2 Measurement test of jujube-material coefficients of restitution

In order to reduce test errors, the pretest was operated by dropping spherical jujube from 600 mm, 800 mm, and 1100 mm respectively, firstly. The result shows that while the drop height is 800 mm, the movement paths of jujubes were all shown in the middle of picture after a rebound, which is convenient for data collection and processing. There H=800 mm was selected as the initial dropping height. Due to the anisotropy of jujube, the movement direction and velocity after rebound are randomized. Ten data which has the closest distance with the normal rebound direction were selected as the valid data, the coefficient of restitution of jujube-steel ($e_{j\text{-}s}$) is 0.35, and jujube-PVC ($e_{j\text{-}p}$) is 0.41. And the rebound heights h_s and h_p are 87.34 mm and 131.74 mm.

3.2 Jujube-material static friction coefficient (μ_s)

According to the standard JB/T 9014.9-1999[40] Determination of External Friction Coefficient of Particulate Material in Continuous Conveying Machines, the jujube-material static friction was determined by the inclined plane method. An apparatus was used to allow sliding to be produced between a particle and a soleplate surface, it is shown in Figure 3. The plate with specific material was settled on the base of the incline instrument. One side of the incline instrument was connected by a rope with the lifting device of the universal testing machine. Adjusting the incline instrument keeping as the horizontal position, after the rope is perpendicular to the incline instrument and keeps the tension, zero the universal testing machine. To prevent jujube rolling, the four jujubes of the same size were pasted and placed 200 mm from the bottom of the plate. Settling the speed of the universal testing machine as 0.01 m/s to lift gradually, the displacement was recorded from the moment of jujube sliding. Each material operated ten times experiment. The mean value has been calculated as the test result.

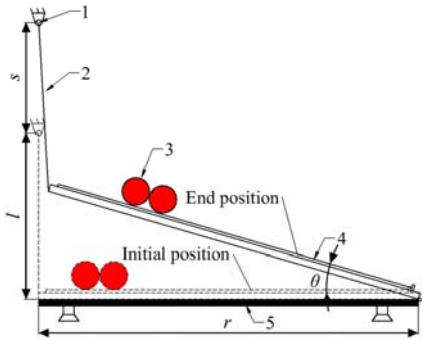

1. Lifting device 2. Tow rope 3. Jujube samples 4. Cantboard 5. Base

Note: r is the length of cantboard, mm; l is the length of the tow rope, mm; s is the rising height of lifting device, mm; θ is the bevel angle of cantboard, (°).

Figure 3 Measurement test of jujube-material static friction coefficient

In order to increase test efficiency and accuracy, the target parameter has been indirectly obtained by the mathematics model after geometric analysis on the test prototype. The geometric relation is given as Equation (3):

$$\mu_s=\arctan(\arctan\frac{l+s}{r}-\arccos\frac{r^2+(s+l)^2+r^2-l^2}{2r\sqrt{(s+l)^2+r^2}}) \tag{3}$$

where, μ_s is the jujube-material static friction coefficient; r is the length of cantboard, mm; l is the length of the tow rope, mm; s is the rising height of lifting device, mm.

Calculating the data via Equation (3). The test was repeated three times and the mean values were calculated for getting an accurate result. Finally, the values of the static friction coefficient and the friction angle of jujube-steel (μ_{ss}, θ_s), were 0.48 and 25.48°, respectively. The values of the static friction coefficient and the friction angle of jujube-PVC (μ_{sp}, θ_s) were 0.64 and 34.1°, respectively.

3.3 Test of jujube-material rolling friction coefficient (μ_r)

The traditional determination method[30-31] has low accuracy due to the jujube, not being the ideal sphere or ellipsoid. In this study, the determination of μ_r is referred to the method of [41]. Based on the conservation of energy principle, it is concluded that the ratio of energy lost by rolling friction to total energy is linear with the residual tangent of bevel angle of cantboard. The gradient is given as μ_r shown in Equation (4).

$$C_f=\frac{W_{fr}}{E_p}=\frac{E_p-E_k}{E_p}\mu r\cot\theta \tag{4}$$

where, C_f is the energy ratio of rolling friction loss, %; W_{fr} is the effort of friction force, J; E_p is the initial gravitational potential energy, J; E_k is the kinetic energy when jujube stop, J; μ_r is the rolling friction coefficient; θ is the bevel angle of cantboard, (°).

Apparatus in Section 2.1 was used in the test. Ten jujubes

with sphericities that were larger than 0.9 were measured according to rolling down from cantboard of six levels at different angles. The result from each level was calculated to obtain the mean value. The linear relation between C_f and $cot\theta$ could be fitted by a linear regression equation. The line gradient is μ_r.

Due to the irregular shape of jujubes, the bouncing or rolling out of the cantboard always happens which is difficult to keep continuous straight rolling on the cantboard. In this case, only the continuous straight rolling section of jujube was selected for calculation. To simplify the calculation, the rectangular coordinate system oxy shown in Figure 4 was established in ProAnalyst, and the jujube centroid trajectory was obtained based on target tracking techniques. The coordinates of the initial frame, end frame as well as two frames after and before the end frame were output as (x_0, y_0), (x_n, y_n), (x_{n-1}, y_{n-1}), (x_{n+1}, y_{n+1}).

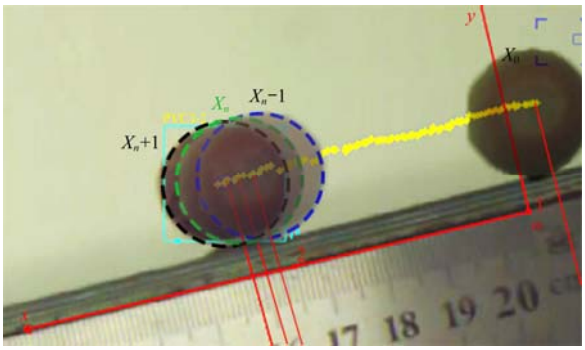

Note: Yellow cross mark is the centroid mark of each frame of jujubes in the continuous straight rolling section; The green, blue and black represents the positions of jujubes at the end frame, the previous and after the end frame respectively; X_0 is the initial frame; X_n is the end frame; X_{n-1} and X_{n+1} are after and before the end frame, respectively.

Figure 4 Coordinate measuring of jujube

Due to the time between two frames being 0.01 s, the rolling distance L could be calculated as,

$$L=x_n-x_0 \tag{5}$$

It is assumed that the n-th frame is the moment of the ends of the jujube rolling, then, the absolute speed of the jujube at n-th frame is V_n, which is given as,

$$V_n=\frac{\sqrt{(x_n-x_{n-1})^2+(y_n-y_{n-1})^2}+\sqrt{(x_{n+1}-x_n)^2+(y_{n+1}-y_n)^2}}{2\Delta t} \tag{6}$$

The C_f of jujube-steel and jujube-PVC in different angles were obtained for linear fitting the relation between C_f and cotθ in Origin 2018, as shown in Figure 5. Meanwhile, the fitted linear Equations (7) and (8) were obtained by linear regression.

$$C_{fs}=0.043\cot\theta+0.030 \tag{7}$$

$$C_{fp}=0.057\cot\theta+0.085 \tag{8}$$

The determinant coefficient R^2 is 0.84 and 0.72 respectively. The rolling friction coefficient of jujube-steel (μ_{rs}) and jujube-PVC (μ_{rp}) were obtained as 0.04 and 0.06.

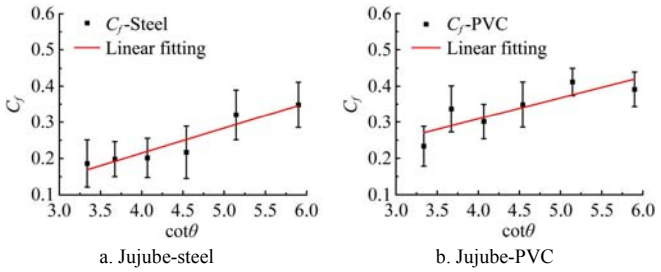

a. Jujube-steel b. Jujube-PVC

Figure 5 Linear fitting of the relation between energy ratios of rolling friction loss and bevel angles of cantboard of jujube-contact materials

As the jujube falls from the incline, the rolling jujube is subjected to gravity, elasticity, and friction at the contact point. Due to the contact between the Jujube and the material surface, both of them have deformation. Jujube is trapped in the supporting surface by gravity. When the jujube rolls forward, the supporting surface in front of the contact is uplifted, and the point of action of the supporting surface on the elastic force of the object is gradually moved forward. It is this elastic force, relative to the center of mass of the object, that produces a torque that prevents the object from rolling. In the test above, when jujube interacts with two kinds of material panels, The PVC panel is easier to deform due to its material inherent characteristics, so the friction coefficient between them is large. In the future, in the design of machinery and equipment such as jujube harvesting and jujube processing, PVC material can be used to control the fluidity of jujube in the relevant parts.

3.4 Repose angle of jujube

The cylinder lifting method[42,43] has been applied for the test on the angle of repose as shown in Figure 6. The inner diameter of the cylinder is 160 mm and the height is 480 mm. In order to ensure the formation of particle pile is only influenced by jujubes interaction, a 400 mm diameter baseplate pasted by jujubes was used as the base. The cylinder which was full of the jujube was settled at the middle of the base.

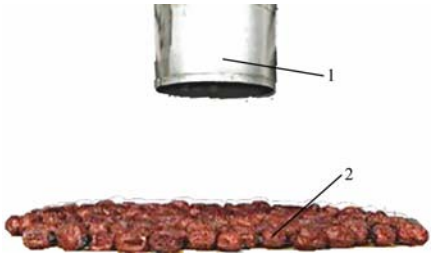

1. Cylinder 2. Base

Figure 6 Physical measurement experiment of the repose angle

Based on pretest results, when lifting speed is 0.02 m/s, the particle group formation has better effectiveness, therefore, lifting the cylinder gradually as 0.02 m/s. The image was collected after the particle group was stable. The results analyzed by Matlab are shown in Figure 7. The test was repeated 10 times. The mean value of angle of repose is 29.88°.

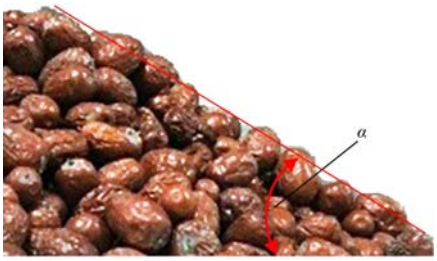

a. Repose angle edge image information extraction

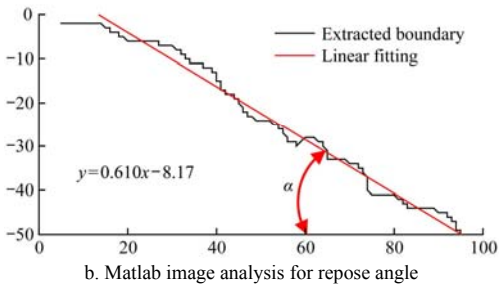

b. Matlab image analysis for repose angle

Note: α is the value of repose angle extracted by repose angle image boundary.

Figure 7 Measurement and extraction of repose angle of jujube pile

4 Simulation and calibration

Based on the physical experiments, the discrete element simulation model of jujube was established. Based on the Hertz Mindlin (no-slip) contact model embedded in EDEM, the simulation contact parameters of jujube-material and jujube-jujube were simulated and calibrated respectively.

4.1 Discrete element simulation model and parameter setting of jujube

The shape characteristics and the size distribution of the particle model directly affect the accuracy of simulation test results[44-46]. Therefore, the multi-sphere polymerization model was used to establish three types of jujube models mentioned in Section 3.1, as shown in Figure 8. The long axis diameter of the ellipsoidal particles a' was set as the measured average length of the long axis a, the minor axis diameter b' was the average length of the short axis $(a+b)/2$, the diameter of spherical-like jujube r' was set as the measured average triaxial diameter $(a+b+c)/3$. Therefore, the long axis diameter of an ellipsoidal particle basic unit is 22.8 mm, the short axis diameter is 19.0 mm, and the diameter of a circular particle basic unit particle is 10.0 mm.

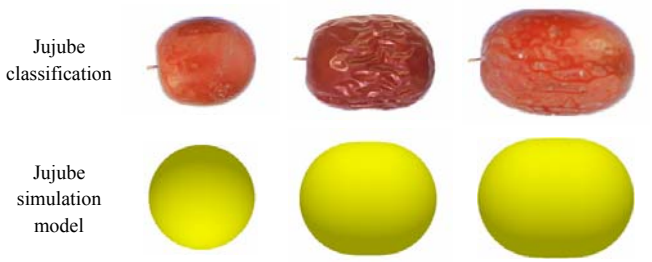

a. Spherical-like b. Small ellipsoidal c. Large ellipsoidal

Figure 8 Classification and simulation model of jujube

Due to Poisson's ratio, elastic modulus and density modulus have no significant effect on the simulation results[47]. In this study, the mean values of each parameter range referenced to [47] and [48] were selected as simulation parameters, which are listed in Table 1.

Table 1 Basic material parameters of simulation test

Material	Poisson ratio	Elastic modulus/Pa	Density/kg·m^{-3}
Jujube	0.40	9.29×10^6	603.5
Steel	0.28	8.2×10^6	7850.0
PVC	0.47	2.0×10^6	1282.0

The research results of reference [41] show that the rolling friction coefficient between particles and contact materials measured by a high-speed camera can be directly used for simulation tests. The same method is used in Section 3.3 of this paper, hence the measured rolling friction coefficient of jujube-material was applied in simulation directly.

4.2 Simulation on coefficient of restitution of jujube-material

Based on the physical test, the spherical-like jujube model was selected for simulation. A particle factory was set 800 mm above the soleplate (the material to be measured), and the particles fall freely at rest. Assuming the impact time is extremely short and the impact force is extremely large during the impact process of spherical particles, other forces could be negligible. In order to protect the interference on test results, the static friction coefficient and rolling friction coefficient between Jujube-material were set to 0.

Settling measured value e_s=0.352, e_p=0.413 as the central level and 5% as the step size, two levels were selected from the upper and lower to complete five groups simulation. The coordinates of particles were derived from EDEM post-processing module for the statistics of rebound height. In order to reduce measurement error, each group of tests was repeated three times and the mean value was calculated. The test result is listed in Table 2.

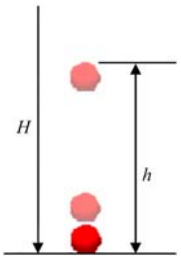

Figure 9 Simulation test of coefficient of restitution

Table 2 Simulation test plan and results of jujube-material coefficient of restitution

Test No.	Steel		PVC	
	Coefficient of restitution x_1	Rebound height y_1/mm	Coefficient of restitution x_2	Rebound height y_2/mm
1	0.39	114.79	0.46	175.16
2	0.37	104.56	0.43	161.50
3	0.35	95.97	0.41	140.18
4	0.33	87.74	0.39	127.19
5	0.32	80.67	0.37	116.41

Note: PVC: Polyvinyl chloride.

With the coefficient of restitution of jujube-contact material as the test factor, and the rebound height as the response value, quadratic polynomial fitting was performed on the results to establish the fitting equation:

$$y_1 = 1446.3x_1^2 - 531.87x_1 + 103.97 \quad (9)$$

$$y_2 = 1751.5x_2^2 - 726.76x_2 + 143.65 \quad (10)$$

The determinate coefficient R^2 of Equations (9) and (10) is 0.999 and 0.992, respectively, indicating that the equation is accurate and effective. By substituting y_1=87.34 mm, y_2=131.74 into the equation, x_1=0.33, x_2=0.39 were solved. To verify the accuracy of the parameters, three simulation tests were carried out by setting the coefficient of restitution of jujube-steel and jujube-PVC as 0.33 and 0.39, respectively. The mean rebound height of particles is 87.30 mm and 130.69 mm, and the relative errors of measured value are 0.04% and 0.8% respectively. It shows that there is no significant difference between the simulation results and the physical test results after calibration. Therefore, the coefficient of restitution of jujube-steel e_s' and jujube-PVC e_p' was determined as 0.33 and 0.39.

4.3 Simulation on static friction coefficient of Jujube-material

In EDEM, the multi-sphere combination method was used to simulate the bonding of four Jujubes (Figure 10a), which was generated by static particle factory at the top of the soleplate. The soleplate was lifted with 0.1 rad/s (Figure 10b). The calibrated value e_s'=0.33, e_p'=0.39 as the coefficient of restitution of Jujube-material was set in this simulation test.

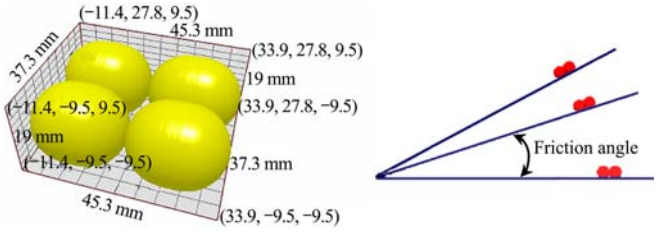

a. Composite particles b. Simulation test

Figure 10 Simulation test of jujube-material coefficient of static friction

With the measured value μ_{ss}=0.48, μ_{sp}=0.64 as the central level and 5% as the step size, two levels were selected from the upper and lower to conduct five groups of simulation. At the end of the simulation, the friction angle was calculated by utilizing the protractor tool in EDEM. Each group of tests was repeated three times and the mean value was calculated for obtaining accurate results. The test results are listed in Table 3.

Table 3 Simulation test plan and results of jujube-material coefficient of static friction

Test No.	Steel		PVC	
	Static friction coefficient x_3	Friction angle y_3/(°)	Static friction coefficient x_4	Friction angle y_3/(°)
1	0.43	24.13	0.74	40.74
2	0.45	25.40	0.71	38.80
3	0.48	26.68	0.68	36.91
4	0.50	28.04	0.64	35.16
5	0.53	29.55	0.61	33.43

With the static friction coefficient of jujube-material as the test factor, and the friction angle as the response value, the result was obtained by quadratic polynomial fitting to establish the fitting equation as follows:

$$y_3 = 48.834x_3^2 + 10.233x_3 + 10.714 \quad (11)$$

$$y_4 = 6.6982x_4^2 + 47.368x_4 + 3.775 \quad (12)$$

The R^2 of Equations (11) and (12) determinate coefficient were both 0.999, indicating that the equation is accurate and effective. By substituting y_3=25.48°, y_4=34.99° into the equation, x_3=0.46, x_4=0.61 were solved. To verify the accuracy of the parameters, three simulations were carried out by setting the friction coefficient of jujube with steel and PVC as 0.46 and 0.61 respectively. The mean friction angle was 25.47° and 35.03°, and the relative errors of measured values were 0.05% and 0.08% respectively. It is demonstrated that the results of the simulation test after calibration are consistent with the physical test. Therefore, the static friction coefficient of jujube-steel μ_{ss}' and jujube-PVC μ_{sp}' were determined as 0.46 and 0.61 respectively.

After calibration, the static friction coefficient of jujube-material in simulation is smaller than that in physical test, and the relative errors are 5.45% and 4.61% respectively. The reason probably is that the jujube simulation model is the smooth spheres instead of micro-wrinkles like the practical jujube surface. The static friction coefficient might be increased due to these wrinkles.

4.4 Calibration of DEM contact parameter of inter-jujube

The contact parameters of the irregular spherical particles such as jujube are difficult to obtain experimentally. The value of the angle of repose is determined by the impact and the sliding and rolling friction between particles, which is usually used to characterize the internal friction of materials[49]. Therefore, based on the physical test, the contact parameters of inter-jujube in the simulation were calibrated through the accumulation simulation test.

4.4.1 Repose angle simulation test

The repose angle simulation model was constructed by using the contact parameters calibrated above, as is shown in Figure 11. Three particle factories were created at the top of the cylinder to generate large ellipsoidal particles, small ellipsoidal particles, and spherical-like particles respectively. In order to reduce the simulation error, the sizes of the 3 jujube particle models generated during simulation were randomly distributed within the range of 0.8-1.4, 1-1.4, 0.8-1.2 times of the particle size of the basic particle unit respectively. The cylinder lifted upward at a constant speed of 0.02 m/s after being filled with particles. Thus, the flow of the particles occurred onto the soleplate due to gravity until a static condition was reached which was given 3 s of simulation time. At the end of the simulation, the images of stable particle pile in $+X$ and $+Y$ views were intercepted, and a digital image analysis method based on Matlab was developed to measure the angle of repose of the stable particle pile. Each group of the test was repeated three times and the mean value was calculated for obtaining the accurate result.

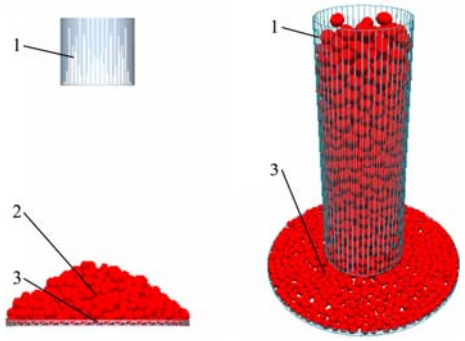

1. Cylinder 2. Particles pile 3. Soleplate

Figure 11 Simulation test of the repose angle of jujube

4.4.2 Box-Behnken test and regression model

The setting of the factors influencing the repose angle (Y) simulation test of the jujube and their level values are listed in Table 4

Table 4 Factor and level of repose angle simulation of jujubes

Level	Coefficient of restitution e (A)	Static friction coefficient μ (B)	Rolling friction coefficient γ (C)
−1	0.2	0.30	0.02
0	0.3	0.45	0.04
1	0.4	0.60	0.06

According to the description on response index and calibration parameters, a response curve test was designed by Box-Behnken in the data processing software Design expert. The simulation test plan is listed in Table 5.

Table 5 Simulation test plan of response angle of jujubes

Test No.	A	B	C	Y/(°)
1	−1	−1	0	28.42
2	1	−1	0	27.89
3	−1	1	0	32.29
4	1	1	0	31.08
5	−1	0	−1	26.43
6	1	0	−1	29.23
7	−1	0	1	32.48
8	1	0	1	28.30
9	0	−1	−1	25.78
10	0	1	−1	27.22
11	0	−1	1	29.54
12	0	1	1	31.35
13	0	0	0	28.16
14	0	0	0	27.78
15	0	0	0	29.11
16	0	0	0	27.75
17	0	0	0	27.98

Note: A represents the coefficient of restitution; B represents the static friction coefficient; C represents the rolling friction coefficient; Y represents the repose angle, (°).

According to the test plan and EDEM simulation, the angle of repose Y under different combination factors was obtained, as shown in Table 5. Variance analysis was performed on the simulation results by Design Expert. The analysis results are listed in Table 6.

Table 6 Result variance analysis of repose angle simulation of jujubes

Variance source	Sum of squares	Mean square sum	F	p
Model	55.77	6.20	10.76	0.0025**
A	1.21	1.21	2.10	0.1904
B	13.30	13.30	23.09	0.0020**
C	21.16	21.16	36.73	0.0005**
AB	0.12	0.12	0.20	0.6677
AC	12.15	12.15	21.08	0.0025**
BC	0.033	0.033	0.058	0.8164
A^2	6.06	6.06	10.52	0.0142*
B^2	1.34	1.34	2.32	0.1716
C^2	0.25	0.25	0.44	0.5303
Residual	4.03	0.58		
Lack of fit	2.79	0.93	2.99	0.1589
Pure error	1.24	0.31		
Cor total	59.81			

Notes: R^2=0.933; R^2adj=0.846; CV=2.63%; Pred R^2=0.224. ** highly significant ($p\leq0.01$); * significant ($0.01<p\leq0.05$).

As shown in Table 6, the p-values of single factor A, B, C, interaction items A^2, B^2, C^2, and AB, AC, BC were analyzed. Single-factor items B, C, and interactive item AC are factors with highly significant influence on Y ($p\leq0.01$), and interactive item C^2 is the factor with significant influence on Y ($p\leq0.05$). The p-value of other factor items is greater than 0.05, so they are all factors with insignificant influence on Y. The significant factors influencing repose angle Y are in descending order of B, A, AC, and A^2. In addition, the obtained model coefficient of the test result is $p<0.01$, the determination coefficient R^2 and the corrected determination coefficient R^2_{adj} are both close to 1, the coefficient of variation CV=2.63%. It is illustrated that the test method is reliable, and the influencing factors A, B, and C have a high degree of interpretation to Y. The second-order response model with a high fitting response degree can be obtained in Equation (13).

$$Y=28.15-0.39A+1.29B+1.63C-0.17AB-1.74AC+0.092BC+1.20A^2+0.56B^2-0.24C^2 \quad (13)$$

4.4.3 Effect analysis of regression model

According to the results of variance analysis of the regression model, the static friction coefficient (B) and the rolling friction coefficient (C) of the single factor items have a significant influence on the angle of repose of jujube ($p<0.01$). As shown in Figure 12, whit the coefficient of restitution increasing, the angle of repose of Jujube decreases first and then increases, while with the increase of static friction coefficient and rolling friction coefficient, the angle of repose shows an overall growth trend, but the growth range is different in different levels. While the factor level is in the range of –1 to 0, the angle of repose increases rapidly under the influence of B. In the range of level 0 to 0.5, the trend of the angle of repose is basically the same under the influence of B and C. In the range of level 0.5 to 1, the angle of repose increases greatly under the influence of C. Within the overall factor level, the rising speed of angle of repose first decreases then increases under the influence of B, and there is a trend of continuous growth. And the variation trend of the angle of repose under the influence of C is opposite to that of B.

According to the second-order response model, three-dimensional response surface and contour map of the interaction ($A\times C$) are shown in Figure 13. When the static friction coefficient (B) is 0.45, the interaction item of the coefficient of restitution (A) and rolling friction coefficient (B) is positive correlation with the repose angle (Y) of jujube. And Y increases with the decrease of A and the increase of C. The rising trend of Y is more significant under the influence of C. The reason is that when the jujube falls out of the cylinder and forms a stable particle pile on the base, the movement of jujubes is mainly impacting and rolling between particles. Due to the decreased coefficient of restitution reducing the kinetic energy after impact, the increased coefficient of rolling friction adds the rolling friction forces generated by the interaction between particles, which is more likely to accumulate. Thus, the angle of repose becomes bigger.

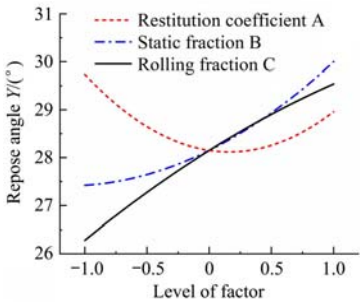

Figure 12 Single-factor response diagram

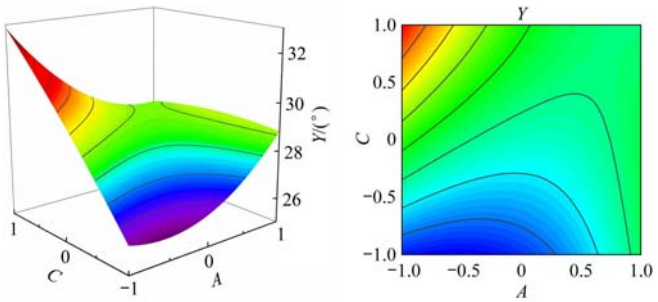

a. Three-dimensional response surface of AC b. Contour map of AC

Note: A represents the coefficient of restitution; C represents the rolling friction coefficient; Y represents the repose angle.

Figure 13 Interaction effect diagram of AC

Figure 14 shows the predicted response and actual scatters of the angle of repose, x-axis and y-axis stand for the actual and predicted value of Y respectively, and the scatters stand for the distribution pattern of predicted Y. In this figure, the predicted scatters are close to the straight line and distributes on two sides of the straight line, which proves that the second-order response model of Y is reliable.

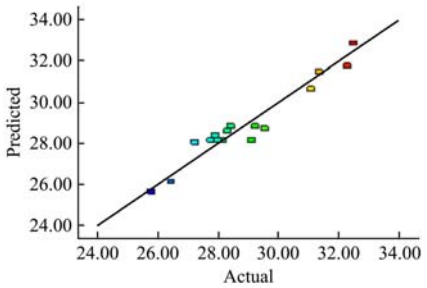

Note: Color points by the actual value of Y.

Figure 14 Predicted responses and actual scatters of the repose angle

4.4.4 Determination of optimum parameter combination and verification test

In order to obtain the optimum parameter combination of the jujube contact parameter in simulation, based on the boundary conditions of the factors listed in Section 4.4.2, the optimization mathematical model was established in Equation (12) through the optimal method of single-objective and multi-objective[32,51,52].

Objective function $Y(A, B, C)$ =29.88°

$$\text{Constraint functions} \begin{cases} 0.20 < A < 0.40 \\ 0.30 < B < 0.60 \\ 0.02 < C < 0.06 \end{cases} \quad (14)$$

where, $Y(A, B, C)$ is the objective function of repose angle of jujube models; A is the coefficient of restitution; B is the static friction coefficient; C is the rolling friction coefficient.

The optimal solution was carried out in the Design-Export software optimization module. After optimization, the simulated contact parameters A, B, and C of jujube were 0.23, 0.33, and 0.04. The value of angle of repose predicted by the model is 29.04°. Then, simulation analysis of the optimized and fit inter-particle contact parameters of the jujube model was conducted in EDEM. The angle of repose was 29.5° and the error was 1.27% compared with the measured value of 29.88°, which is shown in Figure 15b. The contours of the angle of repose from the simulation test and physical test are shown in Figure 15c. Therefore, the verification results of the simulation test are relatively consistent with the measured value.

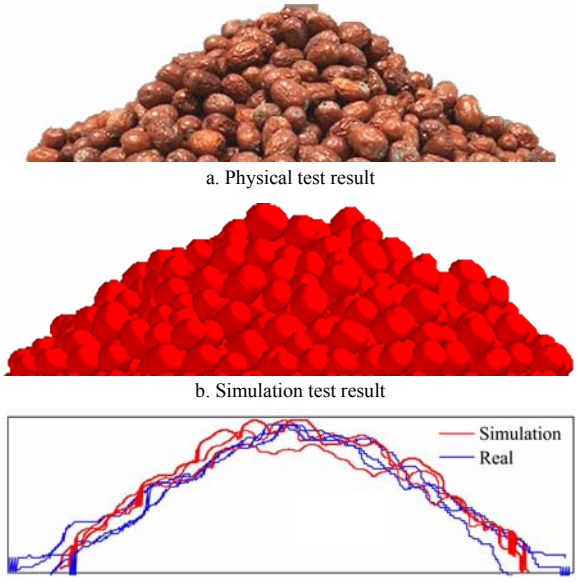

a. Physical test result

b. Simulation test result

c. Boundary fitting of repose angle

Figure 15 Comparison of simulation and experiment result of jujubes

5 Conclusions

1) The contact parameters between jujube and machine components (steel, PVC) were determined by physical test. The coefficient of restitution was 0.35 and 0.41, the static friction coefficient was 0.48 and 0.64, the rolling friction coefficient was 0.04 and 0.06 and the angle of repose was 29.88°.

2) Hertz-Mindlin (no-slip) of discrete element software EDEM was applied to establish a simulation model of jujube. The coefficient of restitution and the static friction coefficient between jujube and machine components (steel, PVC) in the simulation were calibrated. The values of the coefficients of restitution were 0.33 and 0.39, and the static fraction coefficients were 0.46 and 0.61.

3) A response curve test for simulating Y was designed using Box-Behnken function module in Design expert, the test results were subjected to regression variance analysis. The second-order response model for Y was established, and the rule of influences of single factor items and interaction items in the second-order response model on Y was analyzed. It is indicated from the results that the single factors of inter-Jujube particles B and C and the interaction items $A \times C$ have highly significant influences on Y, the interaction items $A \times A$ have significant influences on Y.

4) Based on the second-order response model for Y, the optimal combination of simulation parameters of inter-Jujube particles was obtained by taking the measured value of the physical test as the fitting target. The obtained parameters A, B, and C were 0.23, 0.33, and 0.04. The optimized and fit input parameters of inter-jujube particles were set to a simulation test conducted by EDEM. It is illustrated that the angle of repose Y of the jujube was 29.5°, and the error from measured value 29.88° was 1.27%, which proves the established second-order response model has a high degree of fitting response, and the calibrated parameters are reliable.

5) On the basis of the calibration of input parameters of the jujube, the numerical simulation of the mechanized jujube harvest process could be established through the combination or coupling of EDEM and multidisciplinary categories. It will provide an effective method for analyzing the motion law and contact mechanic characteristics of jujube under the interaction of inter-jujube and jujube-machine components, and theory is provided for harvest principle analysis, harvesting mechanism design, and harvesting components development.

Acknowledgements

The authors acknowledge the support from the National Natural Science Foundation of China (Grant No. 51865050) and the National Key Research and Development Project (Grant No. 2016YFD0701504). In addition, the authors also acknowledge Shujie Han, Bingcheng Zhang, and Xinghua Chen for their help with obtaining experimental data.

[References]

[1] China Agricultural Yearbook Editorial Committee. China agricultural yearbook 2018. Beijing: China Agriculture Press, 2019; 555p. (in Chinese)

[2] Fu L S, Ahmad A, Peng J, Sun S P, Feng Y L, Li R, et al. Harvesting technologies for Chinese jujube fruits: A review. Engineering in Agriculture, Environment and Food, 2017; 10(3): 171–177.

[3] Fu W, Zhang Z Y, Ding K, Cao W B, Kan Z, Pan J B, et al. Design and test of 4zz-4a2 full-hydraulic self-propelled jujube harvester. Int J Agric & Biol Eng, 2018; 11(4): 98–104.

[4] Jing W. Present research and developing measures of the red date harvesting machinery in Xinjiang. Agricultural Science & Technology and Equipment, 2017; 12: 61–63, 66. (in Chinese)

[5] Zhang X J, Bai S G, Jin W, Yuan P P, Yu M J, Yan J S, et al. Development of pneumatic collecting machine of red jujube in dwarfing and closer cultivation. Transactions of the CSAE, 2019; 35(12): 1–9. (in Chinese)

[6] Yu L M, Xu Z, Yang J R, Fan W B, Li N, Long J. Numerical simulation of water and sediment movement in screen filter based on coupled CFD-DEM. Transactions of the CSAM, 2018; 49(3): 303–308. (in Chinese)

[7] Zhu D Q, Li L L, Wen S C, Zhang S, Jiang R, Wu L Q. Numerical simulation and experiment on seeding performance of slide hole-wheel precision seed-metering device for rice. Transactions of the CSAE, 2018; 34(21): 17–26. (in Chinese)

[8] Wang L J, Peng B, Song H Q. Cleaning of maize mixture based on

polyurethane rubber sieve. Transactions of the CSAM, 2018; 49(7): 90–96. (in Chinese)

[9] Nordell L. Particle flow modelling: Transfer chutes and other applications. In: International Materials Handling Conference (BELTCON 9), Johannesburg, South Africa, 1997; Paper No. B09–04.

[10] Lu G, Third J R, Müller C R. Discrete element models for non-spherical particle systems: From theoretical developments to applications. Chemical Engineering Science, 2015; 127: 425–465.

[11] Sinnott M D, Cleary P W. The effect of particle shape on mixing in a high shear mixer. Computational Particle Mechanics, 2016; 3(4): 477–504.

[12] Grima A P, Fraser T, Hastie D B. Discrete element modelling: Trouble-shooting and optimisation tool for chute design. In: BELTCON 16 International Materials Handling Conference, Johannesburg, South Africa, 2011; pp.1–26.

[13] Donohue T, Ilic D, Mcbride W. Comparative particle attrition study for transfer chutes using DEM. In: Continuum and Distinct Element Numerical Modeling in Geomechanics, 2nd International FLAC/DEM Symposium, 2011; Paper No. 15–03

[14] Zhou H, Chen Y, Sadek M A. Modelling of soil-seed contact using the Discrete Element Method (DEM). Biosystem Engineering, 2014; 121: 56–66.

[15] Lai Q H, Zhao J W, Su W, Jia G X, Li J H, Lyu Q. Design and text of air suction directional transplanting device for *Panax notoginseng* seedlings based on DEM-CFD coupling. Transactions of the CSAM, 2021; 52(7): 60–70. (in Chinese)

[16] Wang L J, Peng B, Song H Q. Cleaning of maize mixture based on polyurethane rubber sieve. Transactions of the CSAM, 2018; 49(7): 90–96. (in Chinese)

[17] Boac J M, Ambrose R P K, Casada M E, Maghirang R G, Maier D E. Applications of discrete element method in modeling of grain postharvest operations. Food Engineering Reviews, 2014; 6: 128–149.

[18] Bravo E L, Tijskens E, Suárez M H, Cueto O G, Ramon H. Prediction model for non-inversion soil tillage implemented on discrete element method. Computers and Electronics in Agriculture, 2014; 106: 120–127.

[19] Ma S, Xu L M, Yuan Q C, Niu C, Zeng J, Chen C, et al. Calibration of discrete element simulation parameters of grapevine antifreezing soil and its interaction with soil-cleaning components. Transactions of the CSAE, 2020; 36(1): 40–49. (in Chinese)

[20] Li J W, Tong J, Hu B, Wang H B, Mao C Y, Ma H Y. Calibration of parameters of interaction between clayey black soil with different moisture content and soil-engaging component in northeast China. Transactions of the CSAE, 2019; 35(6): 130–140. (in Chinese)

[21] Ma Z, Li Y M, Xu L Z. Summarize of particle movements research in agricultural engineering realm. Transactions of the CSAM, 2013; 44(2): 22–29. (in Chinese)

[22] Tomar V, Bose M. Anomalies in normal and oblique collision properties of spherical particles. Powder Technology, 2017; 325: 669–677.

[23] Boac J M, Casada M E, Maghirang R G, Harner J P. Material and interaction properties of selected grains and oilseeds for modeling discrete particles. Transactions of the ASABE, 2010; 53(4): 1201–1216.

[24] Horabik J, Molenda M. Parameters and contact models for DEM simulations of agricultural granular materials: A review. Biosystems Engineering, 2016; 147: 206–225.

[25] Gong M. Calibration of material property parameters. Beijing: Report of EDEM user conference, 2013.

[26] Ghodki B M, Patel M, Namdeo R, Carpenter G. Calibration of discrete element model parameters: Soybeans. Computational Particle Mechanics, 2018; 6: 3–10.

[27] González-Montellano C, Fuentes J M, Ayuga-Téllez E, Ayuga F. Determination of the mechanical properties of maize grains and olives required for use in DEM simulations. Journal of food engineering, 2012; 111(4): 553–562.

[28] Ghodki B M, Goswami T K. DEM simulation of flow of black pepper seeds in cryogenic grinding system. Journal of Food Engineering, 2017; 196: 36–51.

[29] Zhang T, Liu F, Zhao M Q, Ma Q, Wang W, Fan Q, et al. Determination of corn stalk contact parameters and calibration of Discrete Element Method simulation. Journal of China Agricultural University, 2018; 23(4): 120–127. (in Chinese)

[30] Liu W Z, He J, Li H W, Li X Q, Zheng K, Wei Z C. Calibration of simulation parameters for potato minituber based on EDEM. Transactions of the CSAM, 2018; 49(5): 125–135,142. (in Chinese)

[31] Wang Y X, Liang Z J, Zhang D X, Cui T, Shi S, Li K H, et al. Calibration method of contact characteristic parameters for corn seeds based on EDEM. Transactions of the CSAE, 2016; 32(22): 36–42. (in Chinese)

[32] Yu Q X, Liu Y, Chen X B, Sun K, Lai Q H. Calibration and experiment of simulation parameters for *Panax notoginseng* seeds based on DEM. Transactions of the CSAM, 2020; 51(2): 123–132. (in Chinese)

[33] Lu F Y, Ma X, Tan S Y, Chen L T, Zeng L C, An P. Simulation calibration and experiment on main contact parameters of discrete elements for rice bub seeds. Transaction of the CSAM, 2017; 48(12): 78–85. (in Chinese)

[34] Liao Y T, Liao Q X, Zhou Y, Wang Z T, Jiang Y J, Liang F. Parameters calibration of discrete element model of fodder rape crop harvest in bolting. Transaction of the CSAM, 2020; 51(6): 73–82. (in Chinese)

[35] Hao J J, Long S F, Li H, Jia Y L, Ma Z K, Zhao J G. Development of discrete element model and calibration of simulation parameters for mechanically-harvested yam. Transactions of the CSAE, 2019; 35(20): 34–42. (in Chinese)

[36] Han Y L, Jia F G, Tang Y R, Liu Y, Zhang Q. Influence of granular coefficient of rolling friction on accumulation characteristics. Acta Physica Sinica, 2014; 63(17): 173–179.

[37] Shi L, Zhao W, Sun B, Sun W. Determination of the coefficient of rolling friction of irregularly shaped maize particles by using discrete element method. Int J Agric and Biol Eng, 2020; 13(2): 15–25.

[38] Wang L J, Zhou W X, Ding Z J, Li X X, Zhang C G. Experimental determination of parameter effects on the coefficient of restitution of differently shaped maize in three-dimensions. Powder Technology, 2015; 284: 187–194.

[39] Yao W L, Yue R. The controversial coefficient of restitution for impact problems. Journal of vibration and shock, 2015; 34(19): 43–48. (in Chinese)

[40] JB/T 9014.9-1999. Determination of external friction coefficient of particulate material in continuous conveying machines. (in Chinese)

[41] Cui T, Liu J, Yang L, Zhang D X, Zhang R, Lan W. Experiment and simulation of rolling friction characteristic of corn seed based on high-speed photography. Transactions of the CSAE, 2013; 29(15): 34–41. (in Chinese)

[42] Wang L J, Li R, Wu B X, Wu Z C, Ding Z J. Determination of the coefficient of rolling friction of an irregularly shaped maize particle group using physical experiment and simulations. Particuology, 2017; 38: 185–195.

[43] Zhang R, Han D L, Ji Q L, He Y, Li J Q. Methods of sandy soil parameters in simulation of discrete element method. Transactions of the CSAM, 2017; 48(3): 49–56. (in Chinese)

[44] Jin F, Xin H L, Zhang C H, Sun Q C. Probability-based contact algorithm for non-spherical particles in DEM. Powder Technology, 2011; 212(1): 134–144.

[45] Cleary P W, Sawley M L. DEM modelling of industrial granular flows: 3D case studies and the effect of particle shape on hopper discharge. Applied Mathematical Modelling, 2002; 26(2): 89–111.

[46] Liu C L, Wang Y L, Song J N, Li Y N, Ma T. Experiment and discrete element model of rice seed based on 3D laser scanning. Transactions of the CSAE, 2016; 32(15): 294–300. (in Chinese)

[47] Wen X Y, Yuan H F, Wang G, Jia H L. Calibration method of friction coefficient of granular fertilizer by discrete element simulation. Transactions of the CSAM, 2020; 51(2): 115–122, 142. (in Chinese)

[48] Fu W, He R, Kan Z, Zhang H M, Wang L H, Yang H Y, et al. Experimental study on mechanical properties of red jujube. Journal of Shihezi University (Natural Science), 2013; 31(4): 518–522. (in Chinese)

[49] Cunha R N, Santos K G, Lima R N, Duarte C R, Barrozo M A S. Repose angle of monoparticles and binary mixture: An experimental and simulation study. Powder Technology, 2016; 303: 203–211.

[50] Guo M, Feng B, Guan Y. Chapter VI: Design and analysis of response face test. In: Experimental Design and Software Application, Beijing: Chemical Industry Press, 2017; pp.137–147. (in Chinese)

[51] Li T H, Huang S H, Niu Z R, Hou J L, Wu Y Q, Li Y H. Optimization and experiment of planting perpendicularity of planetary wheel garlic planter. Transactions of the CSAE, 2020; 36(3): 37–45. (in Chinese)

[52] Li T H, Meng Z W, Ding H H, Hou J L, Shi G Y, Zhou K. Mechanical analysis and parameter optimization of cabbage root cutting operation. Transactions of the CSAE, 2020; 36(7): 63–72. (in Chinese)